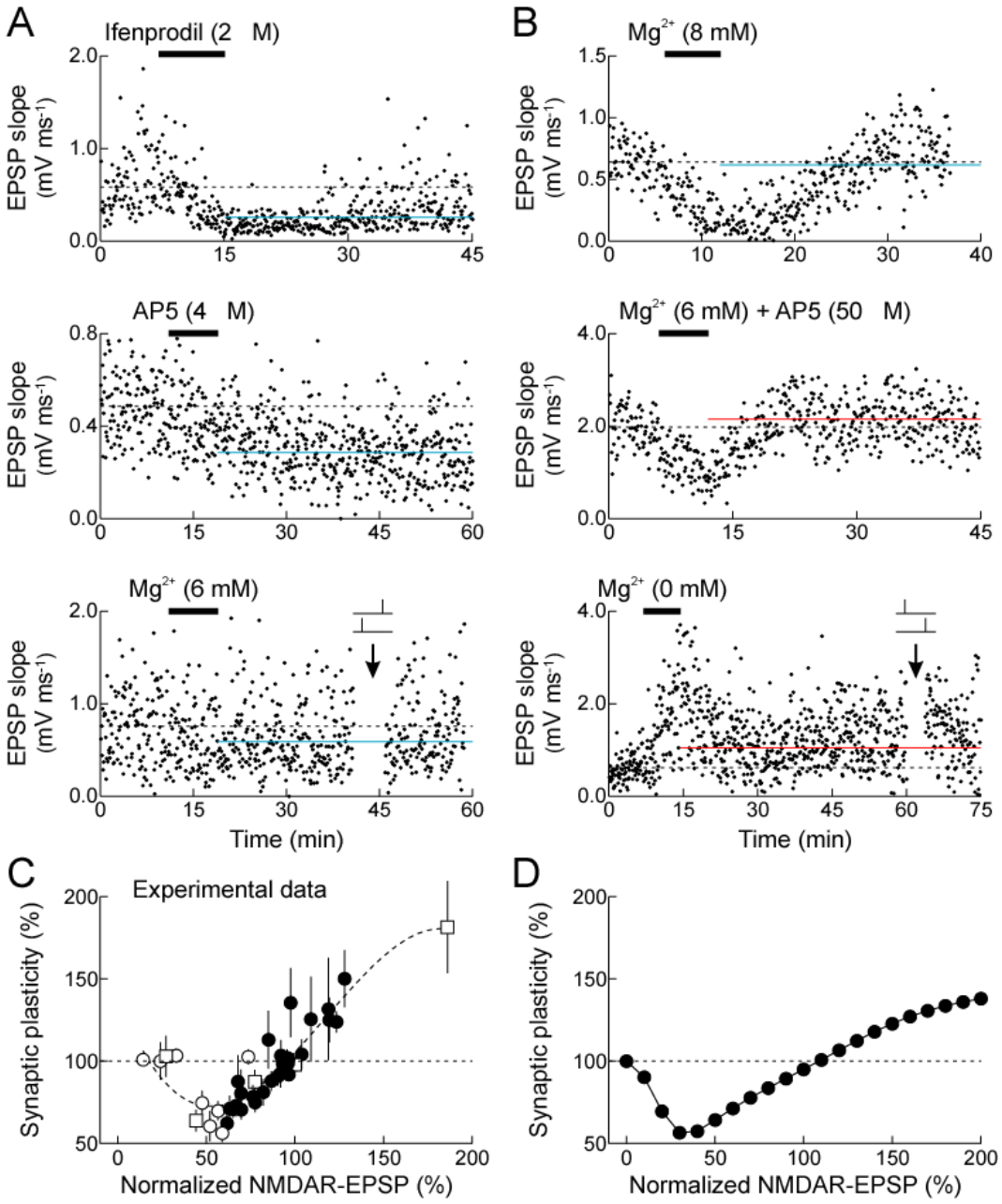

Figure S1. Correlation of NMDARs activity with synaptic plasticity

Supplementary text for Figure S1.

We examined the correlation between the NMDAR-EPSPs and the degree of synaptic modification in both experiments (Fig. S1A-C) and the allosteric model (Fig. S1D). We partially blocked the NMDARs by ifenprodil, a specific inhibitor of NR2B-containing NMDARs, AP5 and high Mg^{2+} (6 mM), and examined the

changes of synaptic strength (Fig. S1A). The partial blockade of NMDARs by these inhibitors resulted in the induction of LTD, and that NMDAR-EPSPs are decreased to ~50% when LTD was induced by these inhibitors (Fig. S1C). We also changed Mg^{2+} and examined the changes of synaptic strength. We found that the induction of LTD is dependent on Mg^{2+} and NMDARs (Fig. S1B). We plotted the NMDAR-EPSPs against long-term synaptic modification in experiments (Fig. S1C) and in the allosteric model (Fig. S1D), and found that the curves both in the experiments and the allosteric model similarly appear biphasic, indicating that the high, moderate, and low NMDAR activity are correlated with potentiation, no-change (neither potentiation nor depression), and depression, respectively. Because Ca^{2+} influx at PSD mainly depends on NMDARs in the allosteric model (see Fig. 9), this suggests the high, moderate, and low Ca^{2+} influx lead to potentiation, no-change (neither potentiation nor depression), and depression, respectively, which is consistent with the idea of three levels of Ca^{2+} for synaptic plasticity (Cho et al., 2001; Froemke et al., 2005; Koester and Sakmann, 1998; Lisman, 2001) and resembles the Bienenstock, Cooper and Munro (BCM) learning rule (Bienenstock et al., 1982) (see also discussion).

Legend

***A*,** Partial block of NMDARs induced LTD. Top, example recording showing that wash-in of ifenprodil (2 μM) induced LTD. Blue line indicates decrease in synaptic strength of –56.3%. Similar results were obtained in three other experiments (LTD: –43.7 ± 5.6%; n = 4, $p < 0.005$). Center, example of LTD induction by AP5 (4 μM). Blue line indicates decrease in synaptic strength of –41.2%. Similar results were obtained in nine other experiments with 2-4 μM AP5 (LTD: –31.0 ± 4.3%; n = 10, $p < 10^{-4}$). Bottom, example of LTD induction by Mg^{2+} (6 mM). Blue line indicates decrease in synaptic strength of –22.4%. Similar results were obtained in three other experiments (LTD: –36.0 ± 6.6%; n = 4, $p < 0.02$). At the time indicated by the arrow, post- → pre-spike pairing (T_{post}

– T_{pre} = –10.6 ms) was repeated for five minutes. No further LTD was induced, suggesting that Mg^{2+}-induced LTD occluded spike-pairing induced LTD. Similar occlusion was observed in all four experiments (change in EPSP slope: 1.8 ± 12.6%; p > 0.8). ***B*****,** Mg^{2+}-induced LTD is dose- and NMDAR-dependent. Top, example showing that wash-in of 8 mM Mg^{2+} had no long-term effect on synaptic strength. Blue line indicates decrease in synaptic strength of –3.6%. Similar results were obtained in two other experiments (change in EPSP slope: 2.9 ± 12.5%; n = 3, p > 0.8). Center, Mg^{2+}-induced LTD is blocked by bath application of AP5 (50 μM). AP5 is in the bath during the duration of the experiment. Red line indicates increase in synaptic strength of 8.9%. Similar results were obtained in two other experiments (change in EPSP slope: 0.1 ± 6.1%; n = 3, p > 0.9). Bottom, example of LTP induction by Mg^{2+} washout (0 mM). Red line indicates increase in synaptic strength of 69.8%. Similar results were obtained in three out of four other experiments (LTP: 86.3 ± 31.9%; n = 5, p < 0.1). At the time indicated by the arrow, pre- → post-spike pairing (T_{post} – T_{pre} = 9.4 ms) was repeated for five minutes. No further LTP was induced, suggesting that 0 Mg^{2+}-induced LTP occluded spike-pairing induced LTP. ***C*****,** Correlation between change in NMDAR-EPSPs and long-term synaptic modification. Summary of all experimental paradigms in which NMDAR suppression and long-term synaptic plasticity were measured: STDP experiments (filled circles), Mg^{2+} wash-in/out (open squares), and NMDAR antagonist wash-in (open circles). There was high correlation between NMDAR suppression and long-term synaptic modification (linear correlation coefficient *r*: 0.994; experiments in which NMDAR suppression was < 50% were excluded). Dashed line represents a third-order polynomial fit to the combined data. ***D*****,** Correlation between change in NMDAR activities and long-term synaptic modification in the allosteric model. NMDARs activity was changed as indicated and the changes of synaptic conductance were plotted. Data were taken at 2 min after the onset of stimulation.

References

Bienenstock EL, Cooper LN, Munro PW (1982) Theory for the development of neuron selectivity: orientation specificity and binocular interaction in visual cortex. J Neurosci 2:32-48.

Cho K, Aggleton JP, Brown MW, Bashir ZI (2001) An experimental test of the role of postsynaptic calcium levels in determining synaptic strength using perirhinal cortex of rat. J Physiol 532:459–466.

Froemke RC, Poo MM, Dan Y (2005) Spike-timing-dependent synaptic plasticity depends on dendritic location. Nature 434:221–225.

Koester HJ, Sakmann B (1998) Calcium dynamics in single spines during coincident pre- and postsynaptic activity depend on relative timing of back-propagating action potentials and subthreshold excitatory postsynaptic potentials. Proc Natl Acad Sci U S A 95:9596–9601.

Lisman JE (2001) Three Ca^{2+} levels affect plasticity differently: The LTP zone, the LTD zone and no man's land. J Physiol 532:285.

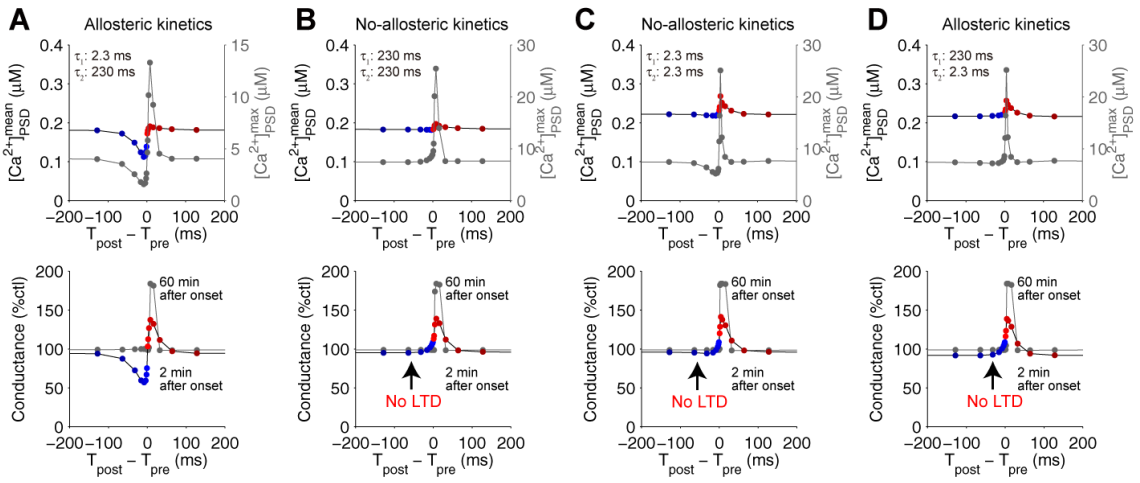

Figure S2. Spike-timing-dependent $[Ca^{2+}]_{PSD}$ (top) and synaptic plasticity (bottom) with the allosteric kinetics of NMDARs. ***A*,** The allosteric model with indicated time constants τ_1 and τ_2. ***B*,** The no-allosteric model with slow suppression. ***C*,** The no-allosteric model with rapid suppression. ***D*,** The allosteric model with the opposite time constants from (***A***). The mean and maximal amplitudes of $[Ca^{2+}]_{PSD}$ were indicated by black and gray, respectively. The synaptic conductance at 2 min and 60 min after the onset of stimulation were indicated by black and gray, respectively. Ca^{2+} permeability of NMDARs $\bar{P}_{NMDAR}$ in the lower panels was set at 0.5, 1, 2.5, and 2.5 $nmol \cdot s^{-1} \cdot mV^{-1} \cdot cm^{-2}$ for (***A***), (***B***), (***C***) and (***D***) respectively, because, with these different $\bar{P}_{NMDAR}$, we can set the same $[Ca^{2+}]_{PSD}^{mean}$ among the all models in order to avoid the induction of potentiation or depression by uncorrelated pre- and post-spiking. This is because the self-suppression of NMDARs by Ca^{2+} influx via NMDARs themselves is dependent on the indicated time constants τ_1 and τ_2. Note that, even if the same $\bar{P}_{NMDAR}$ was used, the similar increase and decrease of $[Ca^{2+}]_{PSD}$ were obtained among the all models, although the uncorrelated pre- and post-spiking induced LTD (data not shown).

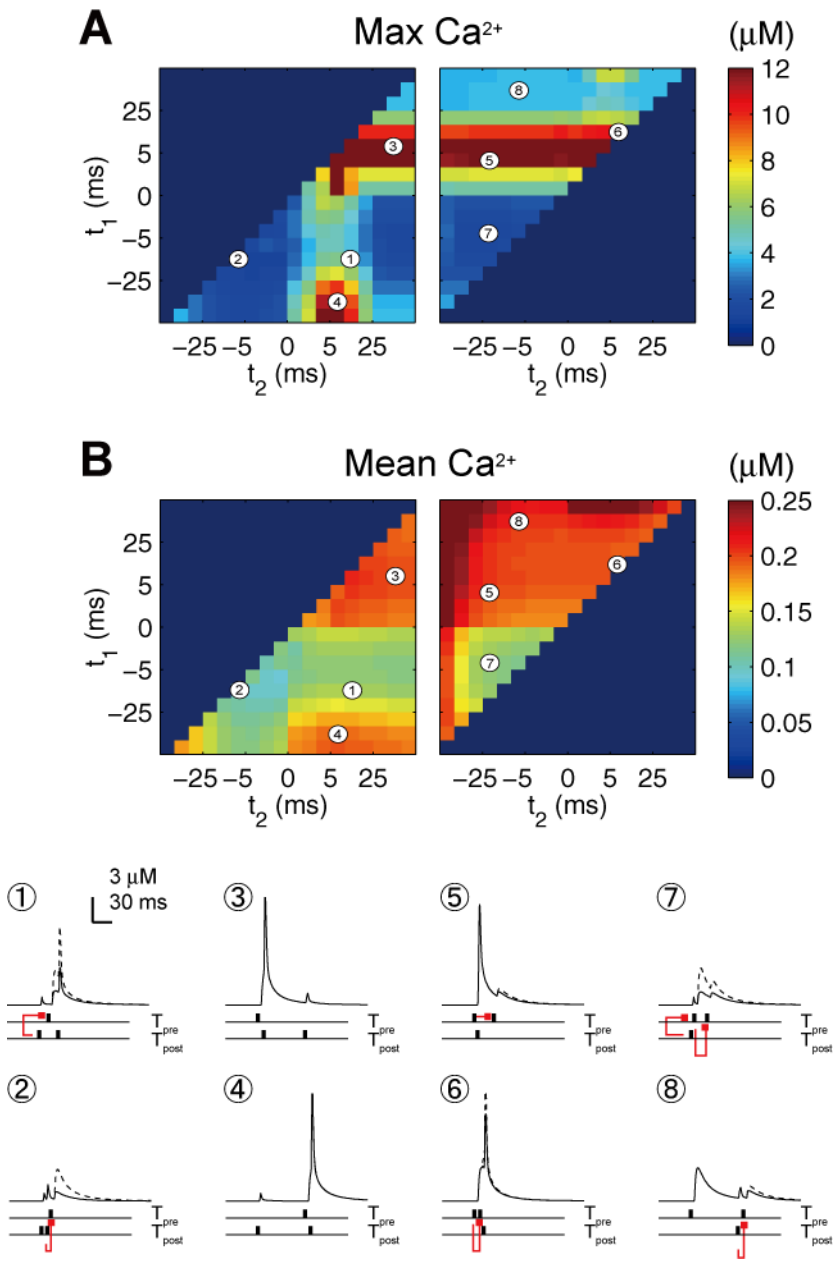

Figure S3. Spike triplet decoding by the allosteric kinetics. The (***A***) maximal amplitude and (***B***) mean of $[Ca^{2+}]_{PSD}$ caused by spike triplets in the allosteric model (100 times pairing, S.E.M. < 0.012 μM for the max, S.E.M. < 3.16×10^{-4} μM for the mean). Two post- and one pre-spikes (left) and one post- and two pre-spikes (right). Typical Ca^{2+} influx in the numbered areas is shown. The dashed lines indicate the Ca^{2+} influx in the no-allosteric model with slow

suppression (τ = 230 ms). The red lines indicate the suppression of NMDARs by prior pre- and post-spiking. With two post- and one pre-spikes, potentiation was induced by pre- $\rightarrow$ post- $\rightarrow$ post-spiking or by post- $\rightarrow$ (long interval) pre- $\rightarrow$ post-spiking, both of which triggered high Ca^{2+} influx (areas 3 and 4). In contrast, depression was induced by post- $\rightarrow$ post- $\rightarrow$ pre-spiking or by post- $\rightarrow$ pre- $\rightarrow$ post-spiking, both of which triggered low Ca^{2+} influx (areas 1 and 2). This result agrees with the earlier experimental observation (Froemke and Dan, 2002). With one post- and two pre-spikes, potentiation was induced by the pre- $\rightarrow$ post- $\rightarrow$ pre-spiking, except for the pre- $\rightarrow$ (long interval) post- $\rightarrow$ pre-spiking or by the pre- $\rightarrow$ pre- $\rightarrow$ post-spiking, both of which triggered high Ca^{2+} influx (areas 5 and 6). In contrast, depression was induced by the post- $\rightarrow$ pre- $\rightarrow$ pre-spiking or by the pre- $\rightarrow$ (long interval) post- $\rightarrow$ pre-spiking, which triggered low Ca^{2+} influx (areas 7 and 8). This is also, in principle, consistent with the previous observation (Froemke and Dan, 2002).

Reference

Froemke RC, Dan Y (2002) Spike-timing-dependent synaptic modification induced by natural spike trains. Nature 416:433–438.

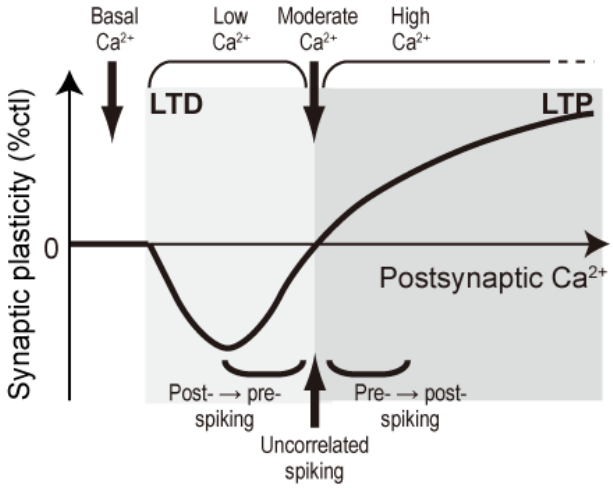

Figure S4. Schematic representation of three Ca^{2+} hypothesis. In the allosteric model, we set the pre- → post-spiking, the uncorrelated spiking, and the post- → pre-spiking induced the high, moderate, and low Ca^{2+} influx, which led to potentiation, no change (neither potentiation nor depression), and depression, respectively (supplemental Fig. 1C, available at www.jneurosci.org as supplemental material; Koester and Sakmann, 1998; Cho et al., 2001; Lisman, 2001; Froemke et al., 2005).

References

Koester HJ, Sakmann B (1998) Calcium dynamics in single spines during coincident pre- and postsynaptic activity depend on relative timing of back-propagating action potentials and subthreshold excitatory postsynaptic potentials. Proc Natl Acad Sci U S A 95:9596-9601.

Cho K, Aggleton JP, Brown MW, Bashir ZI (2001) An experimental test of the role of postsynaptic calcium levels in determining synaptic strength using perirhinal cortex of rat. J Physiol 532:459-466.

Lisman JE (2001) Three Ca2+ levels affect plasticity differently: the LTP zone, the LTD zone and no man's land. J Physiol 532:285.

Froemke RC, Poo MM, Dan Y (2005) Spike-timing-dependent synaptic plasticity depends on dendritic location. Nature 434:221-225.

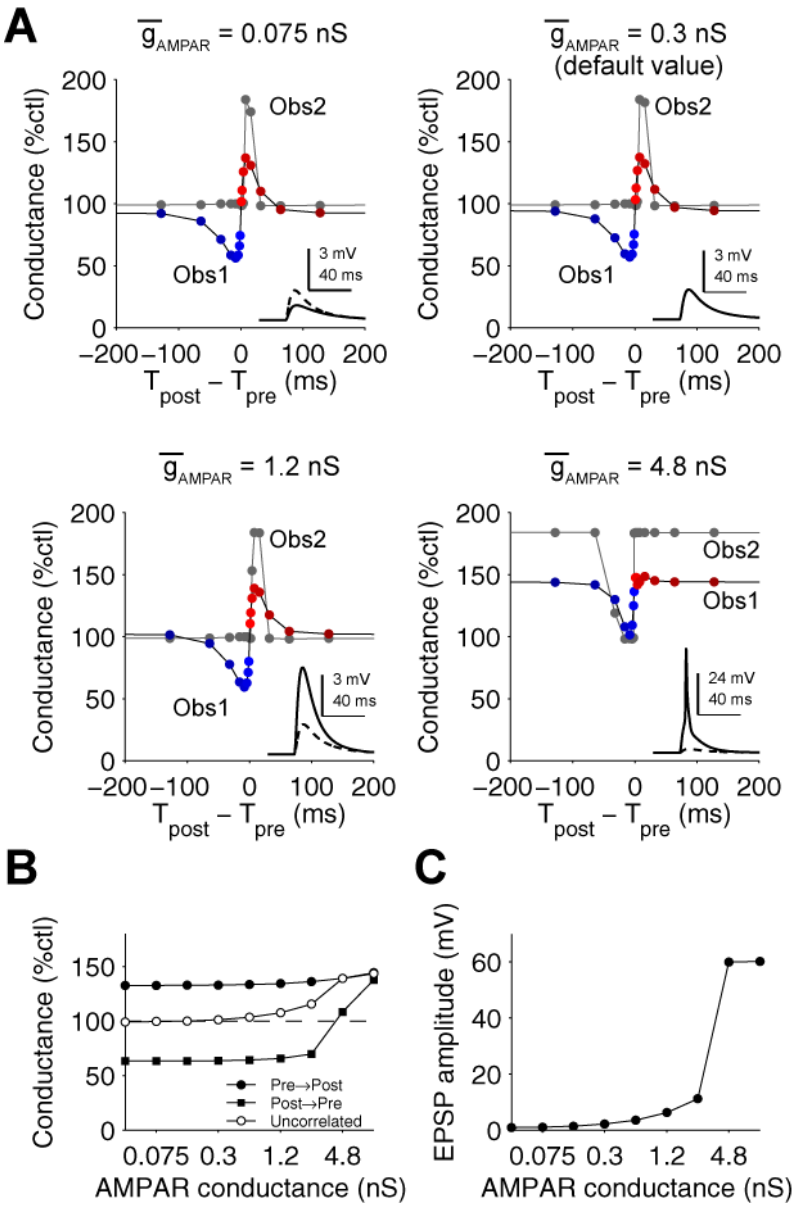

Figure S5. AMPAR-conductance dependency of STDP.

Supplementary text for Figure S5.

We analyzed the sensitivity of the amplitude of STDP against the conductance of AMPARs With pre- → post-spike-timing, the amplitudes of LTP were almost the same against the changes of the conductance of AMPARs, and with post- → pre- or uncorrelated spike-timings, the amplitudes almost remained the same until a pre-spike evokes the dendritic action potential (< 2.4 nS). When a

pre-spike evokes the dendritic action potential (> 2.4 nS), a pre-spike alone induced sufficient NMDARs activation, resulting in the LTP, whose amplitude is the same as that of LTP induced by pre- → post-spiking.

Legend

***A*,** Spike-timing- dependent synaptic conductance in the allosteic model at 2 min (obs 1) and 60 min (obs 2) after onsets of stimulation with the indicated $\bar{g}_{AMPAR}$. The default $\bar{g}_{AMPAR}$ is 0.3 nS. Insets show EPSPs with the indicated $\bar{g}_{AMPAR}$ (solid lines) and EPSPs with the default $\bar{g}_{AMPAR}$ (dashed lines). ***B*,** AMPAR-conductance dependency of synaptic plasticity induced by pre- → post-spiking, post- → pre-spiking and uncorrelated spiking. Data were taken at 2min after onsets of stimulation. The intervals between pre-spiking and post-spiking are 8 ms (pre → post), –8 ms (post → pre), and–256 ms (uncorrelated). ***C*,** AMPAR-conductance dependency of EPSP amplitude induced by a pre-spike.